

15 August 1995

DOE/ER/45510--T/

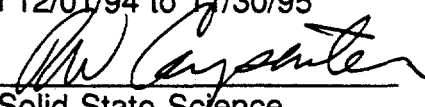
RECEIVED

OCT 06 1995

OSTI

Progress Report: Grant DE-FG03-94ER45510

"High Resolution Interface Nanochemistry and Structure"
for the period 12/01/94 to 11/30/95

PI: R.W. Carpenter 
Center for Solid State Science
Arizona State University
Tempe, AZ 85287-1704
No unexpended funds

I. Experimental Results

A. Materials

1. Ceramic interfaces and grain boundaries

A comprehensive paper describing our measurements of *chemical widths* and *structural widths* at heterophase interfaces and matrix grain boundaries in silicon nitride matrix/silicon carbide whisker reinforced ceramic matrix composites will appear in the November 1995 issue of the Journal of the American Ceramic Society (1). An early draft of this was sent to your office last year. The objective of the work was determination of the final spatial distribution of elements from the $Al_2O_3 + Y_2O_3$ sintering aids in the grain boundary and whisker/matrix interface regions after densification processing at $1780^\circ C$. Prior to this work boundaries and interfaces in ceramics have been characterized only by high resolution imaging (HREM), which often showed thin amorphous films to exist in those regions. The width of these films is called the boundary/interface structural width. Free energy of mixing considerations indicated that oxygen, aluminum and yttrium would be expected to dissolve to some extent into the silicon nitride and silicon carbide crystals bounding interfaces/boundaries if atomic mobilities were high enough during processing despite limited solubility, to form chemical widths at boundaries/interfaces that are expected to affect properties. Main conclusions from our results are:

- Observed chemical widths were 10 to 120 times greater than structural widths for both matrix grain boundaries and heterophase interfaces after 1 hour at $1780^\circ C$.
- Chemical widths were laterally continuous along grain boundaries but discontinuous along heterophase interfaces. The discontinuous distributions along the SiC/Si₃N₄ interfaces were caused by near atomically sharp steps about 100Å high on the SiC whisker surfaces that made direct high pressure contact with the Si₃N₄ matrix crystals during densification processing. The steps were blunted by preferential Gibbs-Thompson dissolution during processing, but not eliminated. The spaces between the blunted steps along the processed heterophase interfaces contain the chemical widths. These discontinuities will result in a lateral spatial variation in bond strength between the silicon carbide whisker reinforcements and the nitride matrix grains along these interfaces.
- Chemical widths extended further into Si₃N₄ than into SiC. Chemical widths were usually symmetric at nitride grain boundaries, i.e. the grain boundaries were mirror planes for the chemical distributions. They were not symmetric at nitride/carbide interfaces.
- The chemical widths were diffusion controlled and processing dependent in these non-equilibrium microstructures. Chemical width magnitudes showed that solute diffusion coefficients in the Si₃N₄ and SiC crystals were in the range of 10^{-15} to 10^{-17} cm²/sec at $1780^\circ C$.

We first observed chemical widths in ceramics through measurements of oxygen and nitrogen distributions at boundaries/interfaces using the position resolved electron energy loss (PREELS) method developed on this research grant. The presently attainable spatial resolution for this method is about 20Å. To completely determine chemical widths in these

DISCLAIMER

Portions of this document may be illegible in electronic image products. Images are produced from the best available original document.

ceramics the yttrium, aluminum and silicon distributions must also be measured. Yttrium, with atomic number 39, is much heavier than all other elements in the chemical widths. Its more complex electronic structure makes energy loss measurements of its chemical width difficult to interpret. However, its relatively high atomic weight, compared to all other elements in the distributions, gives it a much larger high angle elastic electron scattering cross section (Rutherford scattering for angles greater than about 70 mrad). For this reason we used high angle dark field elastic imaging to determine the yttrium chemical widths. Some of these results are shown in fig. 7 of ref. 2 (pre-print enclosed). This high angle imaging method is chemically sensitive through its contrast dependence on atomic number but is not spectroscopic. Fig. 7 of ref. 2 shows our experimental confirmation, using x-ray emission spectroscopy, that the yttrium chemical width was correctly measured by the high angle dark field z-contrast method. We have now successfully applied this method to heavy element chemical width measurements at both grain boundaries and heterophase interfaces in ceramics for the first time. We also used small probe characteristic x-ray emission spectroscopy to determine that the aluminum chemical width followed that of oxygen and yttrium and was of similar magnitude (see Fig. 7 of ref. 2).

Most recently we have used our Zeiss 912 Omega filter Analytical TEM (obtained with DOE/URI grant DE-FG05-91ER79302, PIs J.M. Cowley, R.W. Carpenter et al.) to examine oxygen, nitrogen, aluminum and silicon distributions in Si_3N_4 matrix grain boundaries of these composites. These results are shown in fig. 8 of ref. 2 and in reference 3 (reprint enclosed). These energy selected transmission electron microscopy images (ESTEMI) show that the grain boundary chemical widths are enriched in oxygen and aluminum and depleted in nitrogen and silicon, in excellent agreement with our light element position resolved nanospectroscopy results. The magnitude of the chemical widths determined by ESTEMI were smaller than the same widths determined by small probe nanospectroscopy. This difference is a consequence of the much lower incident electron current per unit area on the specimen for ESTEMI than that for high current density small probe nanospectroscopy, as discussed in refs. 2 and 3. We have not yet applied ESTEMI to heterophase interfaces but our grain boundary results indicate that useful results will be obtained.

Our applications of position resolved electron energy loss nanospectroscopy, z-contrast imaging, ESTEMI, x-ray emission point nanospectroscopy and HREM are leading to understanding the emerging relationships between chemical and structural widths for ceramics. Chemical widths should always be greater than or equal to structural widths and anion chemical widths should always be matched to cation chemical widths. The latter rule follows from the different effective valences of oxygen and nitrogen, and of silicon, aluminum and yttrium, to maintain electrical neutrality.

2. Metal/ α (6H)-SiC(0001) interfaces.

We have used our methods for chemical and structural width measurement to investigate as-deposited and thermally reacted interfaces between Ti or Pt and vicinal Si-terminated (0001) SiC single crystals during the last year. Research on these materials is collaborative with Prof. Bob Davis' research group at North Carolina State University, who are synthesizing these interfaces. Our current results for Ti/SiC interfaces are given in reference 4 (reprint enclosed). After room temperature MBE deposition, Ti/SiC interfaces are epitaxial and atomically flat and sharp. The chemical width is equal to the structural width because the atomic mobilities of all species present were too low to form a larger chemical width. After thermal treatment at 700°C interface reaction had occurred, and a reaction zone containing TiC and Ti_5Si_3 formed between the Ti and SiC. We determined that chemical widths greater than the corresponding structural widths formed at all interfaces between these phases. These results are consistent with our observations for ceramic interfaces, and illustrate the applicability of our interface analysis methods to materials research in general. During this research we observed subunit cell contrast in HREM images of the hexagonal phases present (6H-SiC, α -Ti and Ti_5Si_3) that may have been related to the existence of non-zero

chemical widths in these phases. We conducted an extensive investigation of its origin, discussed below.

Our results for Pt/6H-SiC showed that the interface in specimens deposited at room temperature again is chemically and atomically sharp because atomic mobility in both phases was low. This interface was not epitaxial, however. After reaction treatment at elevated temperature a complicated multiphase reaction zone containing a platinum silicide and other phases formed. Some of these results are shown in figs. 1-3 of reference 2. After reaction treatment at 650°C an asymmetric chemical width was observed at the interface extending into the SiC, but not into Pt (fig. 1 of ref. 2). Isolated reaction zones extending into the SiC were also observed (fig. 2 of ref. 2). After thermal treatment at 750°C an extensive reaction zone that penetrated into the SiC had formed (fig. 3 of ref. 2). The SiC interface remained largely flat, but contained large steps or superledges. Apparently the reaction proceeds by lateral propagation of superledges formed at reaction zones such as the one shown in fig. 2 of ref. 3. A manuscript describing these results in detail is in preparation.

There is a fundamental difference in reaction zone morphology between Ti/SiC where both stable carbide and silicide are formed, and Pt/SiC where only a stable silicide is formed. The product phase interfaces in the Pt/SiC case are often smoothly curved (fig. 3, ref. 2) indicating local melting may have occurred, whereas all interfaces remain flat in the Ti/SiC case (ref. 4) indicating that a solid state reaction occurred. The difference between these two reaction mechanisms is an important topic for future research as noted below.

3. Oxygen distributions in monolithic SiC.

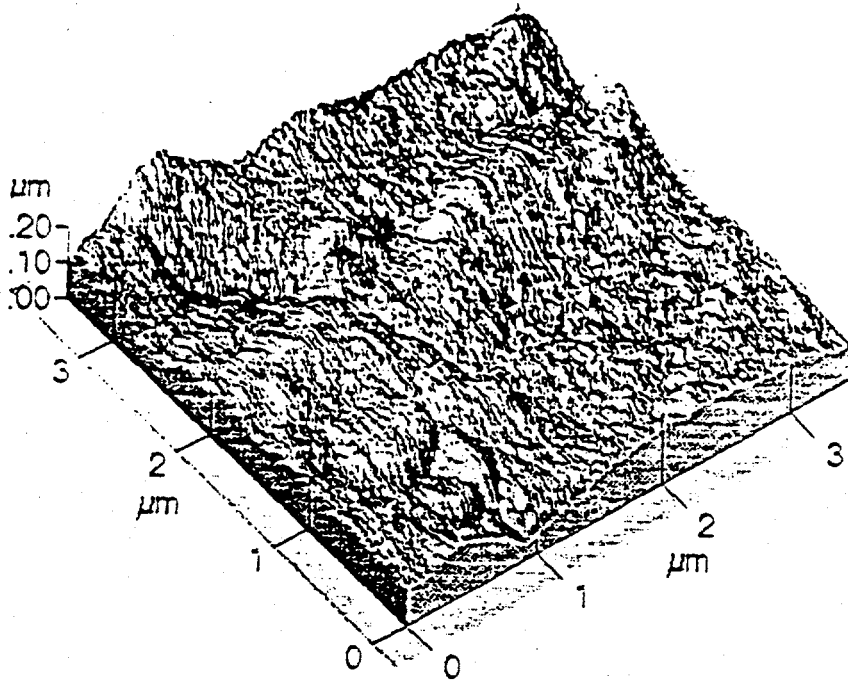
A paper describing our measurements of oxygen distributions in a variety of SiC ceramics has been published and a reprint is enclosed (reference 6).

4. We have begun to apply our experimental interface analysis methods to other SiC/nitride and metal on nitride interfaces. Our first results for aluminum and gallium nitride are shown in ref. 5 (copy enclosed).

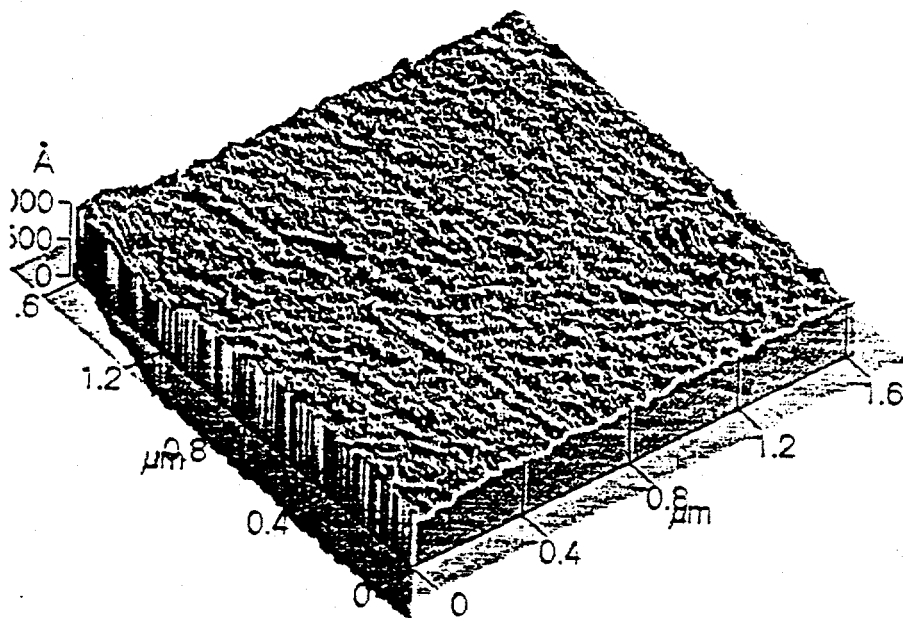
B. Experimental Methods

1. Local thickness variations at Interfaces/Boundaries.

We have noted earlier that local thickness variations in TEM specimens, in the form of grooves at intersections of boundaries/interfaces with specimen surfaces caused by differential ion milling, will make quantitative measurements of composition variations at boundary/interface chemical widths very difficult. To recover the true composition profile from a position resolved nanospectroscopy chemical width plot of a grooved specimen both the focused probe current density distribution and the local thickness variation must be deconvoluted from the experimental data. Two problems make this apparently simple procedure very difficult: (1) it is very difficult to detect boundary/interface grooves in a TEM image, and (2) it is essentially impossible to measure thickness profile at the groove by any transmission method when a composition variation (chemical width) exists, especially when an amorphous phase or disordered region exists at the groove. Development of a specimen preparation method that eliminates grooving is by far the preferred solution. This development requires use of an experimental method that will detect and measure the depth of surface grooves on a TEM specimen to assess success. We spent significant effort on these two very difficult problems this year, and the results obtained so far are excellent. First, we developed a mechanical polishing method for thinning ceramic composites known to contain non-zero chemical widths to electron transparency, to find a thinning method that would not cause the differential thinning attributed to ion milling. Second, we investigated bright and dark field optical microscopy, Nomarski phase contrast optical microscopy, high resolution field emission SEM, and atomic force scanning probe microscopy to measure TEM specimen surface roughness. The latter proved the most useful. Two of our results appear in the figures below. The upper figure is the surface of an ion milled TEM ceramic composite specimen.



Ion Milled



Mechanical Polish

The intersection of three matrix grain boundaries at a triple junction intersecting the surface is visible near the middle of the image. The peak to valley height difference on this surface is 2122Å, the RMS surface roughness is 308Å and the average surface roughness is 241Å. The lower image is the same specimen material, but thinned by the mechanical polishing method mentioned above. No grain boundaries or interfaces are visible intersecting this specimen surface but the size of the imaged area is larger than the matrix grain size, so it is likely that boundaries do intersect the imaged surface. The peak to valley height difference on this surface is 152Å, the RMS roughness is 38Å and the average roughness is 31Å. This specimen also has a large electron transparent thin area. This remarkable result shows great promise for producing specimens suitable for quantitative measurement of composition variations (chemical widths) across interfaces/boundaries.

2. Interface Synthesis

We have synthesized planar interfaces of Cu/Al₂O₃, austenitic stainless steel/austenitic stainless steel, and austenitic stainless steel/Ti/austenitic stainless steel using our prototype planar interface synthesis unit. We are presently analyzing the structural and chemical microstructure of these interfaces by TEM. First results indicate that the interfaces in stainless steel are chemically clean. We have completed the design of our primary planar interface synthesis machine, using our experience with the prototype unit to refine our design. All components of the primary machine have been ordered, most have arrived, and construction has begun. Design and construction of the primary unit is funded by DOE/URI grant DE-FG-05-93ER79234; PIs R.W. Carpenter, M.J. Kim et al.

II. Theory Results

A. Subunit cell alternating contrast in HREM images of hexagonal crystals

During our investigation of Ti/6H-SiC interfaces we noticed that HREM images of hexagonal phases in this material system exhibited bands of alternating bright/dark contrast with repeat distance smaller than the unit cells of the hexagonal phases. Preliminary results of these observations were given in an extended conference abstract last year. The hexagonal phases that exhibited the effect were 6H-SiC itself, alpha-Ti, and Ti₅Si₃. The cubic reaction product in the system, TiC, did not exhibit the effect. This effect has been observed by other authors in HREM images of 6H-SiC and attributed by them to various causes: (1) the crystal being tilted slightly off a low index zone axis when the HREM images were taken, or (2) violation of dynamical extinction rules permitting excitation of forbidden Bragg reflections which should cause the alternating contrast, or (3) solute absorption affects causing subtle changes in crystal structure that would induce the alternating contrast. The origin of the alternating contrast is clearly a complicated and important question. Since we are involved in high resolution chemical width measurement, and the chemical width *is* solute absorption, we decided to perform a detailed theoretical investigation of the source of this alternating contrast in all of the hexagonal phases we examined in the Ti/6H-SiC material system. The results are in ref. 7 (preprint enclosed). Clear examples of the alternating bright/dark contrast in experimental 6H-SiC HREM images are given in figs. 1,2 of ref. 7. To gain physical insight into the mechanism responsible for this contrast effect we constructed computer crystal models using CERIUS software on a Silicon Graphics platform for each of the hexagonal phases and viewed them along the exact HREM image zone axis and at slight tilts off the zone axis. It was apparent that slight off-axis tilts changed electron channeling conditions in *part* of the unit cells, but left channeling conditions relatively unchanged in the remainder of the cell. This tilting effect is anisotropic, i.e. it depends on tilt azimuth as well as magnitude, as shown for 6H-SiC in figs. 3-5 of ref. 7, but the tilt magnitudes required to induce the contrast effect in HREM images of the phases turn out to be very small, ~0.5 mrad. The crystal models were used to simulate HREM images of the hexagonal phases as a function of tilt, azimuth, and specimen thickness, and the results were in excellent agreement with experimental HREM images as shown in figs. 6-11 of ref. 7. Digital diffractograms, computed from experimental HREM images of the hexagonal phases that exhibited the alternating contrast effect, did indeed exhibit excited forbidden Bragg reflections, as shown in fig. 12 of ref. 7. Similar models

constructed for cubic phases TiC and beta-SiC and the corresponding computed images did not exhibit alternating contrast, which agreed with the absence of that contrast in experimental images. The crystallographic symmetry elements responsible for the alternating contrast behavior of the hexagonal phases are evident from table 1 of ref. 7: they are the six fold screw axes and c-glides common to all three hexagonal phases. These elements are absent in the space groups of the cubic phases examined. Note that it was not necessary to invoke any chemical width-induced changes in crystal symmetry of the hexagonal phases, caused by solute absorption, to explain the alternating contrast effect in their HREM images; it is purely an effect of their space group symmetry and the incident electron beam direction (tilt) during imaging. The crystal models showed *why* the alternating contrast occurs when the necessary point group symmetry elements are present. This contrast increases with specimen thickness for tilted hexagonal crystals. It does *not* appear at *any* specimen thickness if the crystals are *not* tilted. This contrast is to be expected in tilted images of other crystals containing appropriate symmetry elements. We may assume then that the solutes absorbed during formation of chemical widths form random substitutional solid solutions in these hexagonal crystals but do not change their basic symmetry. More information about the magnitude of this effect can be obtained by computing projected potentials and the amplitudes and phases of diffracted beams contributing to their HREM images as functions of crystal tilt and specimen thickness. That remains as a future project. We are now beginning to use this HREM simulation method on triad interfaces as shown in ref. 8 (copy enclosed).

B. Boundary and interface structure

We have refined our quantum molecular dynamics (QMD) calculations for coincidence grain boundaries in silicon bicrystals and attempted to apply this method to heterophase interfaces, particularly Ti/6H-SiC interfaces, for which we have excellent experimental results. This theoretical effort has not been successful yet, because sufficiently accurate Ti wave functions are not yet available and because the computational requirements of the method are too severe. The super-cell size upper limit for this method (and most similar theoretical techniques) is 200 to 300 atoms. We are finding that super-cells of 1000 or more atoms are required for atomistic simulation of a heterophase interface by this method. We want to pursue the Ti/6H-SiC (and similar interface problems) further since high resolution electron microscopy experimental results alone cannot prove whether the Ti is bonded to Si atoms or C atoms alone or shares bonding between Si and C atoms at the interface. We are now evaluating a self-consistent tight binding cluster method for the total energy calculation that may remove the difficult Hamiltonian matrix diagonalization problem with the super-cell method. We have established a collaboration with Dr. M. Kohyama (Dept. of Materials Physics, Osaka National Research Institute, Japan) to help with this work. He has used a similar method to successfully calculate grain boundary structures in SiC and also Si.

C. Small electron probe nanospectroscopy of interfaces and grain boundaries

We have developed a deconvolution method for separating the current density distribution in small focused electron probe from a chemical distribution, i.e. from a chemical width at an edge-on grain boundary or heterophase interface measured by position resolved nanospectroscopy. Used with specimens prepared without local thickness variations, this should permit us to recover undistorted chemical width profiles and quantitative composition variations across boundaries and interfaces.

D. Near edge fine structure in electron energy loss spectra

We have completed theoretical calculations of aluminum L_{2,3} core edges from Al metal and Al in Al₂O₃ and AlN. These results will be published in the coming year. The results are in agreement with our earlier theoretical interpretation of near edge fine structure in Si, SiC, Si₃N₄ and SiO₂. The main changes occur because Al or Si bonding to the non-metal constituents becomes more ionic across each series of compounds from the element to the oxide. A publication describing the results is in preparation.

III. References from this Project

1. Chemical and Structural Widths of Interfaces and Grain Boundaries in Silicon Nitride-Silicon Carbide Whisker Composites, K. Das Chowdhury, R.W. Carpenter, W. Braue, J. Liu and H. Ma. J. Amer. Cer. Soc. (Nov. 1995)
2. Local Chemistry at Interfaces and Boundaries: Ceramic and Electronic Composite Materials, R.W. Carpenter, J.S. Bow, M.J. Kim, K. Das Chowdhury and W. Braue, to appear in Microscopy, Microanalysis and Microstructures, preprint enclosed.
3. Chemical Widths at Composite Interfaces: Relationships to Structural Widths and Methods for Measurement, R.W. Carpenter, J.S. Bow, M.J. Kim, K. Das Chowdhury, and W. Braue, Mater. Res. Soc. Symp. Proc. Vol. 357, 271-276 (1995), reprint enclosed.
4. Chemistry, microstructure, and electrical properties and interfaces between thin films of titanium and alpha (6H) silicon carbide (0001), L.M. Porter, R.F. Davis, J.S. Bow, M.J. Kim, R.W. Carpenter and R.C. Glass, J. Mater. Res. 10, 668-679 (1995), reprint enclosed.
5. An HREM study of the microstructure of Al contact on GaN/AlN/SiC thin films. Y. Huang, L. Smith, M.J. Kim, R.W. Carpenter and R.F. Davis, Mater. Res. Soc. Symp. Proc. Vol. 355, 433-439 (1995), copy enclosed.
6. Oxygen Sinks in SiC-Based Ceramics, W. Braue, K. Das Chowdhury and R.W. Carpenter, Mater. Res. Soc. Symp. Proc. Vol. 327, 275-280 (1994), reprint enclosed.
7. Crystallographic Origin of the Alternate Bright/Dark Contrast in 6H-SiC and Other Hexagonal Crystal HREM Images, J.S. Bow, R.W. Carpenter and M.J. Kim, submitted to J. Micros. Soc. Amer., preprint enclosed.
8. HREM Image Simulation of $Ti_5Si_3/TiC/6H-SiC$ Interfaces, J.S. Bow, R.W. Carpenter and M.J. Kim. Proc. 52nd Ann. Mtg. Micros. Soc. Amer., 518 (1995), reprint enclosed.

*Copies of reprints/preprints
not included here, but sent
to grant monitor in Germantown
RWC*

DISCLAIMER

This report was prepared as an account of work sponsored by an agency of the United States Government. Neither the United States Government nor any agency thereof, nor any of their employees, makes any warranty, express or implied, or assumes any legal liability or responsibility for the accuracy, completeness, or usefulness of any information, apparatus, product, or process disclosed, or represents that its use would not infringe privately owned rights. Reference herein to any specific commercial product, process, or service by trade name, trademark, manufacturer, or otherwise does not necessarily constitute or imply its endorsement, recommendation, or favoring by the United States Government or any agency thereof. The views and opinions of authors expressed herein do not necessarily state or reflect those of the United States Government or any agency thereof.